

## A mouse model of luciferase-transfected stromal cells of giant cell tumor of bone

Carol P. Y. Lau<sup>1</sup>, Kwok Chuen Wong<sup>1</sup>, Lin Huang<sup>2</sup>, Gang Li<sup>1</sup>, Stephen K.W. Tsui<sup>3</sup>, and Shekhar Madhukar Kumta<sup>1</sup>

<sup>1</sup>Department of Orthopaedics and Traumatology, The Chinese University of Hong Kong, Shatin, NT, Hong Kong, <sup>2</sup>Department of Surgery, Prince of Wales Hospital, Shatin, NT, Hong Kong, and <sup>3</sup>School of Biomedical Sciences, The Chinese University of Hong Kong, Shatin, NT, Hong Kong

### Abstract

A major barrier towards the study of the effects of drugs on Giant Cell Tumor of Bone (GCT) has been the lack of an animal model. In this study, we created an animal model in which GCT stromal cells survived and functioned as proliferating neoplastic cells. A proliferative cell line of GCT stromal cells was used to create a stable and luciferase-transduced cell line, Luc-G33. The cell line was characterized and was found that there were no significant differences on cell proliferation rate and recruitment of monocytes when compared with the wild type GCT stromal cells. We delivered the Luc-G33 cells either subcutaneously on the back or to the tibiae of the nude mice. The presence of viable Luc-G33 cells was assessed using real-time live imaging by the IVIS 200 bioluminescent imaging (BLI) system. The tumor cells initially propagated and remained viable on site for 7 weeks in the subcutaneous tumor model. We also tested *in vivo* antitumor effects of Zoledronate (ZOL) and Geranylgeranyl transferase-I inhibitor (GGTI-298) alone or their combinations in Luc-G33-transplanted nude mice. ZOL alone at 400 µg/kg and the co-treatment of ZOL at 400 µg/kg and GGTI-298 at 1.16 mg/kg reduced tumor cell viability in the model. Furthermore, the anti-tumor effects by ZOL, GGTI-298 and the co-treatment in subcutaneous tumor model were also confirmed by immunohistochemical (IHC) staining. In conclusion, we established a nude mice model of GCT stromal cells which allows non-invasive, real-time assessments of tumor development and testing the *in vivo* effects of different adjuvants for treating GCT.

### Keywords

Giant cell tumor of bone, stromal cells, animal model, zoledronate, geranylgeranyl transferase-I inhibitor

### History

Received 4 March 2015  
Revised 8 July 2015  
Accepted 15 July 2015  
Published online 1 September 2015

### Introduction

Giant cell tumor of bone (GCT) is a common neoplasm in Chinese patients, constituting 20% of all benign bone tumors (1). The tumor usually affects young adults between the ages of 20–40 and is typically located at the articulating ends of the long bones such as the distal femur proximal tibia, the humerus and even the pelvis. GCT is treated with intralesional curettage and local adjuvants but is prone to recurrence with reported rates ranging from 0% to 65% (2,3). Wide resection of GCT can reduce the rate of local recurrence but the surgical procedure requires the sacrifice of a larger segment of the bone, necessitating an obligatory reconstruction of the bone defect or a large prosthetic reconstruction of the whole joint, eventually compromising limb function. GCT is also largely unresponsive to systemic chemotherapy that has systemic toxicity and even potential life-threatening side effects. Given that GCT is a benign bone tumor, we aim to

achieve an adequate local tumor clearance but yet maximally preserve the surrounding normal bone for better limb function. Therefore, adjuvant therapies for GCT, i.e. bisphosphonates have been investigated (4,5). Bisphosphonates have been shown to not only decrease the rate of tumor recurrence but also exert anti-tumor effect, leading to tumor stabilization and less aggressive recurrence. Consequently, subsequent need of repeated surgeries and the scale of each surgery is reduced.

We have previously shown that a combination of the bisphosphonate, Pamidronate (PAM) with a protein prenylation inhibitor, Geranylgeranyl transferase-I inhibitor (GGTI-298) results in a dual inhibition of cell viability and proliferation in the GCT stromal cells, may partly through suppressing the protein prenylation pathways (6). Further animal studies are warranted before clinical application, however, the difficulty of replicating an animal model of GCT is well known. When GCT stromal cells were subcutaneously injected into immunocompromised mice, they did not recruit monocytes and induce giant cell formation (7–9). Some studies showed that, when GCT tissues were implanted into subcutaneous area or thigh muscle of athymic nude mice, the implants induced formation of a shell of new bone enclosed

Correspondence: Shekhar Madhukar Kumta, Department of Orthopaedics and Traumatology, The Chinese University of Hong Kong, Rm 09A31, 9/F, Main Clinical Block and Trauma Centre, Prince of Wales Hospital, Shatin, NT, Hong Kong. Tel: +852-26323947. E-mail: kumta@cuhk.edu.hk

by the host vascularized fibrous tissue (10,11), and the tumor tissue was resorbed up to 35 days post-transplantation. We have developed instead an alternative model in which the GCT stromal cells continue their neoplastic proliferation by using a three-dimensional (3D) hydrogel to deliver the luciferase-transduced GCT stromal cells either subcutaneously on the back or to the tibiae of the nude mice. The 3D matrix provided a well-contained, growth-enhancing environment in which the tumor cells initially propagated and remained viable; and the luciferase transduction of the GCT stromal cells allowed real-time, non-invasive bioluminescence imaging of the tumor growth. This shall provide an invaluable platform for studying the *in vivo* effects of drugs on the neoplastic cells of the GCT.

## Methods

### Reagents

Zoledronate (ZOL) was purchased from Novartis Pharmaceuticals Ltd. (Basle, Switzerland). Geranylgeranyl transferase-I inhibitor (GGTI-298) was purchased from Sigma (St. Louis, MO). A 0.8 mg/ml stock solution of ZOL in phosphate buffered saline (PBS) and an 11.6 mg/ml stock solution of GGTI-298 in dimethyl sulfoxide (DMSO) were kept at  $-80^{\circ}\text{C}$  until use. The stock solution of ZOL and GGTI-298 were freshly diluted in saline before administration. Cell culture medium was purchased from Invitrogen Life Technologies (Carlsbad, CA). Other chemicals and reagents were of analytical grade.

### Primary culture of GCT stromal cells and other cells

The study was approved by the local ethics committee (Prince of Wales Hospital). GCT specimens were collected from patients after surgery. Primary culture of GCT stromal cells was established as previously described (6), and maintained at  $37^{\circ}\text{C}$  and 5%  $\text{CO}_2$  in Dulbecco's Modified Eagle Medium (DMEM) containing 10% fetal bovine serum (FBS), 1% penicillin–streptomycin–neomycin (PSN; Invitrogen). Bone marrow mesenchymal stem cells (MSC) obtained from a healthy donor were used as the control cells for evaluation in the drug toxicity test. GCT stromal cell has been reported to be of the MSC origin (12,13). MSC were isolated by the method as previously described (14) and cultured in DMEM containing 10% FBS and 1% PSN. Human monocytes, THP-1 cells were purchased from ATCC, and re-suspended with completed RPMI1640 medium supplemented with 10% FBS and 1% PSN. The cells were then cultured at  $37^{\circ}\text{C}$  in a humidified atmosphere of 5%  $\text{CO}_2$  and 95% air.

### Virus production and luciferase gene transduction of GCT stromal cells

Lentiviral particles were produced in 293T cells by calcium phosphate-mediated transfection involving a four-plasmid expression system. In brief, 293T cells were plated into  $10\text{ cm}^2$  plates at  $2 \times 10^6$  cells/plate for 24 h, and chloroquine (Sigma) was added to the medium at a final concentration of  $25\ \mu\text{M}$ . The transfer vector plasmid (Lenti CMV/TO V5-LUC) obtained from Addgene (Cambridge, MA), the helper plasmids plp-1 and plp-2, and the envelope plasmid

plp-VSVG were mixed with calcium chloride (0.25 M) and HEPES-buffered saline (HBS), and were added into the 293T cells. The virus particles in the medium were harvested at 72 h after transfection, concentrated by PEG-it virus precipitation solution (System Biosciences, San Francisco, CA). GCT stromal cell line G33 was transduced with the V5-LUC Puro expression lentivirus vector containing the luciferase gene coding region and the puromycin resistant gene, in the presence of polybrene (Sigma). The culture medium was changed to the complete medium supplemented with 10% FBS and 1% PSN, 17 h after addition of lentivirus. Stable cells were selected in the culture medium supplemented with puromycin. The resulting cell line is referred to Luc-G33.

### 3-(4,5-Dimethylthiazol-2-yl)-2,5-diphenyltetrazolium bromide (MTT) assay

GCT stromal cells (G33), luciferase transduced G33 cells (Luc-G33) and MSC were seeded at 7000 cells/well in 96-well plates individually. The three cell lines were treated with ZOL (0–1.6  $\mu\text{g}/\text{ml}$ ) and GGTI-298 (0–23.2  $\mu\text{g}/\text{ml}$ ) alone, respectively, for 5 days. These dose ranges were selected according to our previous studies (6,15). For the combination treatment, three combinations were used: 0.4  $\mu\text{g}/\text{ml}$  ZOL + 5.8  $\mu\text{g}/\text{ml}$  GGTI-298, 0.8  $\mu\text{g}/\text{ml}$  ZOL + 11.6  $\mu\text{g}/\text{ml}$  GGTI-298; and 1.6  $\mu\text{g}/\text{ml}$  ZOL + 23.2  $\mu\text{g}/\text{ml}$  GGTI-298. 3-(4,5-dimethylthiazol-2-yl)-2,5-diphenyltetrazolium bromide (MTT) solution at 0.5 mg/ml was added into the cultured cells, followed by incubation at  $37^{\circ}\text{C}$  for 3 h in a  $\text{CO}_2$  incubator. The absorbance at 540 nm was measured using a microplate reader (Bio-rad 3550).

### *In vitro* bioluminescent imaging (BLI) for cell viability

Prior to implantation, cell viability and presence of luciferase-transduced GCT stromal cells (Luc-G33 cells) were assessed using *in vitro* bioluminescent imaging (BLI). Luc-G33 cells were seeded at 7000 cells/well in 96-well black-color plates for 24 h and treated with single ZOL (0–1.6  $\mu\text{g}/\text{ml}$ ) and GGTI-298 (0–23.2  $\mu\text{g}/\text{ml}$ ) treatment respectively for 5 days. For combined treatments, the drugs were added at the three fixed concentrations as described in the MTT assay. After treatment, the culture medium was replaced with fresh medium containing D-luciferin potassium salt at 150  $\mu\text{g}/\text{l}$  (Xenogen, Alameda, CA) and incubated further at  $37^{\circ}\text{C}$  and 5%  $\text{CO}_2$  for 10 min and then subjected to BLI by the IVIS 200 BLI (Xenogen, Alameda, CA). The effect of the combined treatments was analyzed using the combination index (CI), as described by Chou and Talalay (16).  $\text{CI} < 1$ ,  $= 1$  and  $> 1$  indicate a synergism, additive effect and antagonism, respectively. CI values were then used to estimate the dose reduction index (DRI) for combination of drugs. DRI is a measure of how many folds the dose of each drug in a synergistic combination may be reduced at a given effect level when compared with the dose of each drug alone (17).

### Monocytes migration assay

Human monocytes (THP-1 cells) were seeded at a  $7 \times 10^5$  cells/well density in the upper compartment of transwell chambers (6.5 mm diameter, 8 mm pore size; Corning Costar, Pittsburgh, PA). The lower chambers contained 600  $\mu\text{l}$  of

DMEM plus 10% FBS and 1% PSN; in the absence of the GCT stromal cells (control), or in the presence of G33 cells or Luc-G33 cells at a  $5 \times 10^4$  cells/well density, respectively. The transwell chambers were incubated at 37 °C in air with 5% CO<sub>2</sub> and THP-1 cells were allowed to migrate for 120 min toward the lower chamber. Non-migrated cells were scraped off from the upper surface of the membrane with a cotton swab. Migrated cells remaining on the bottom surface were fixed with freshly prepared 4% paraformaldehyde, and counted after staining with crystal violet solution. The total number of cells on each membrane was counted from five random fields of view.

### Cell proliferation assay

G33 and Luc-G33 cells, respectively, were seeded on 96-well plates (7000 cells/well) for 72 h. The cell proliferation rate was measured by BrdU incorporation using the Cell Proliferation ELISA, BrdU (colorimetric) kit (Roche Diagnostics, GmbH, Mannheim, Germany) according to the manufacturer's instructions.

### Preparation of synthetic extracellular matrix for cell transplantation

Luc-G33 cells were resuspended in serum-free medium at  $2 \times 10^7$  cells/ml for each 100 µl injection with hydrogel. The hydrogel concentration was optimized and each 30 µl of cell suspension was mixed with 35 µl of Glycosil and 35 µl of Gelin-S to form a 70% synthetic hydrogel solution using an Extracel-X Hydrogel Kit (Glycosan BioSystems Inc., Salty Lake City, UT). The resulting cell suspension was mixed by gentle pipetting and supplemented with 20 ng/ml murine RANKL and 4 ng/ml murine vascular endothelial growth factor (VEGF) (Peprotech, Rocky Hill, NJ). In the end, 17.5 µl of Extralink was added to the cell suspension immediately before injection to the animals.

### Transplantation of luciferase-expressing GCT stromal cells in nude mice and the drug treatment

All the animal experiments were carried out under approval by the animal experimental ethics committee of the Chinese University of Hong Kong (CUHK). Forty male (8–9 weeks old) nude mice were obtained from the Laboratory Animal Services Centre (LASEC) of CUHK. The nude mice were initially weighed and anesthetized intraperitoneally with 10% chloral hydrate at 0.1 ml/30 g live weight. The operative area was prepared with iodine. Each mouse was then given an intraosseous ( $1 \times 10^6$ ) and a subcutaneous injection ( $3 \times 10^6$ ) of Luc-G33 cells in hydrogel into the tibia and under the dorsal skin, respectively. A preliminary study had been proceeded on eight mice for observing the duration of the BLI signals from the Luc-G33 cells in the mice *in vivo*. Thirty-two mice after Luc-G33 implantation were randomly divided into four groups (8 mice/group) with equal average body weight and drugs were given to each mice three days after cell injection. Group 1 was then given 0.9% sodium chloride (Abbott) as the vehicle control treatment; Groups 2–4 were given ZOL and GGTI treatments at the following dosages: group 2 treated with ZOL alone at 400 µg/kg; group 3 with

GGTI-298 alone at 1.16 mg/kg; and group 4 with the combination of ZOL at 400 µg/kg and GGTI-298 at 1.16 mg/kg. The doses used for GGTI-298 are clinically relevant (18,19). Although the dose for ZOL is relatively high when compared with the dose used for treating animal bone resorption models (e.g. 100 µg/kg), but it is a moderate dose for treating animal cancer models such as prostate cancer and breast cancer and it is well tolerated in nude mice (20–22). Drugs were administered subcutaneously, twice per week for four weeks. The mice were euthanized at day 35 after cell-implantation.

### Whole-body real-time BLI

The presence of viable Luc-G33 cells in the nude mice was assessed using real-time live imaging by the IVIS 200 BLI system (Xenogen). The substrate D-luciferin potassium salt was injected into the intra-peritoneal cavity at 150 mg/kg body weight (30 mg/ml), approximately 10 min before imaging. Mice were anesthetized using isoflurane/oxygen and placed on the imaging stage. Images were collected in 10–30 s. The photon emission transmitted from mice was captured and quantitated in photons/s using Living Image software version 2.50 (Caliper Life Sciences Inc., Hopkinton, MA).

### Histological and immunohistochemical (IHC) examinations

The tibiae and skin collected from the nude mice were fixed, embedded and processed for tissue sectioning. The tibiae were decalcified in 9% formic acid for 2 weeks prior to paraffin embedding. The specimens were sectioned (5 µm) and stained with hematoxylin and eosin (H&E). For immunohistochemical (IHC) staining of human Luc-G33 cells in the tibia and skin samples, tissue sections (5 µm) were de-waxed in xylene and then rehydrated in sequentially diluted ethanol followed by PBS rinse as previously described (14) with minor modifications. In brief, monoclonal mouse antibody raised against human mitochondrial protein (Abcam, Cambridge, UK) was applied at a dilution of 1:400 in 1% BSA–PBS for incubation at 4 °C overnight. After stringent washing in PBS twice, a secondary antibody conjugated to horse radish peroxidase (HRP) was used for further incubation. Diaminobenzidine (DAB) as chromogen was used for color development. Slides were finally counterstained with hematoxylin and examined under a light microscope. Quantitative analysis was performed with ImmunoRatio (23), which analyzes immunostained slides using color deconvolution for stain separation and adaptive IsoData algorithm for thresholding.

### Statistical analysis

Single drug treatments and combined treatment were compared with the control using the analysis of variance (ANOVA), and Dunnett's multiple comparison test was used as the post-hoc test;  $p < 0.05$  was considered statistically significant. The difference between the cell proliferation rate of G33 cells and Luc-G33 cells was analyzed by student t-test. A log transformation was applied on the BLI measurements to

stabilize the variances. Two-way ANOVA and Sidak's multiple comparisons test were used to analyze the data obtained from before and after treatments in animal experiments.

## Results

### ZOL, GGTI-298, and the co-treatment reduced cell viability of MSC and GCT stromal cells in MTT assay

Single treatments with ZOL or GGTI-298 and the co-treatment reduced cell viability in MSC, G33 and Luc-G33 in a dose-dependent manner (Figure 1A–C). Significant inhibition was observed at 0.8–1.6  $\mu\text{g/ml}$  for ZOL; and at 5.8–23.2  $\mu\text{g/ml}$  for GGTI-298, respectively. For the combined treatment, the three combinations 0.4  $\mu\text{g/ml}$  ZOL + 5.8  $\mu\text{g/ml}$  GGTI-298; 0.8  $\mu\text{g/ml}$  ZOL + 11.6  $\mu\text{g/ml}$  GGTI-298; and 1.6  $\mu\text{g/ml}$  ZOL + 23.2  $\mu\text{g/ml}$  GGTI-298, significantly inhibited cell viability in the three cell lines. ZOL had a stronger effect on inhibiting cell viability in MSC than in GCT stromal cells at concentration of 1.6  $\mu\text{g/ml}$  (Figure 1A); in contrast, GGTI-298 had a greater inhibition in GCT stromal cells than in MSC at concentrations of 5.8  $\mu\text{g/ml}$  and above (Figure 1B). Luc-G33 cells were less sensitive in response to single treatments with ZOL (only at concentration of 0.8  $\mu\text{g/ml}$ ) or GGTI-298 (at concentrations of 5.8  $\mu\text{g/ml}$  and 11.6  $\mu\text{g/ml}$ ), respectively, when compared with the wild-type G33 cells. However, there was no significant difference between Luc-G33 cells and G33 cells in drug sensitivity in the co-treatment (Figure 1C).

### Cell viability of Luc-G33 in luciferase assay

Luc-G33 cells showed strong BLI signals and the maximum radiance was  $5.11 \times 10^6$  p/s/cm<sup>2</sup>/sr (Figure 2A). ZOL and GGTI-298 reduced cell viability in Luc-G33 cells in a dose-dependent manner (Figure 2B and C). A significant inhibition was observed with ZOL and GGTI-298 treatment alone at 0.8  $\mu\text{g/ml}$  and 5.8  $\mu\text{g/ml}$ , respectively. The IC<sub>50</sub> (drug concentration at which it induces 50% growth inhibition) was  $1.50 \pm 0.37$   $\mu\text{g/ml}$  for ZOL, and  $5.41 \pm 0.59$   $\mu\text{g/ml}$  for GGTI-298 in the 5-day treatment. Combination of ZOL with GGTI-298 led to synergistic inhibition and the cell viability was reduced and ranged from 25.97% to 0.17% of the controls under the low (0.4  $\mu\text{g/ml}$  ZOL + 5.8  $\mu\text{g/ml}$  GGTI-298) to high (1.6  $\mu\text{g/ml}$  ZOL + 23.2  $\mu\text{g/ml}$  GGTI-298) concentration treatment conditions (Figure 2D). The low concentration co-treatment showed a mild synergistic effect (CI =  $0.94 \pm 0.18$ ); and the high concentration demonstrated a strong synergistic effect (CI =  $0.66 \pm 0.12$ ). Dose reduction indices (DRIs) for the low concentration co-treatment were 6.75 for ZOL, and 1.30 for GGTI-298; and the high concentration were 25.41 for ZOL, and 1.65 for GGTI-298.

### Characterization of luciferase-transduced GCT stromal cells

The luciferase-transduced GCT stromal cells, Luc-G33 cells were characterized by cell proliferation and recruitment of monocytes. There was no significant difference between the wild type G33 cells and Luc-G33 cells in terms of cell proliferation rate assessed by BrdU incorporation assay.

The cell proliferation rate of G33 cells and Luc-G33 cells were  $2.36 \pm 0.25$  and  $2.16 \pm 0.18$ , respectively (Figure 3A). Moreover, there was also no significant difference in the ability of recruiting monocytes by G33 cells and Luc-G33 cells through the transwell system. The number of migrated monocytes was  $40.33 \pm 11.65$  and  $41.07 \pm 13.56$  for the lower compartment containing G33 cells or Luc-G33 cells respectively. Only  $9.53 \pm 5.06$  number of monocytes was found on the control (Figure 3B), which was significantly less than that of the lower compartments with G33 cells or Luc-G33 cells.

### A new animal model of luciferase-expressing GCT stromal cells in nude mice

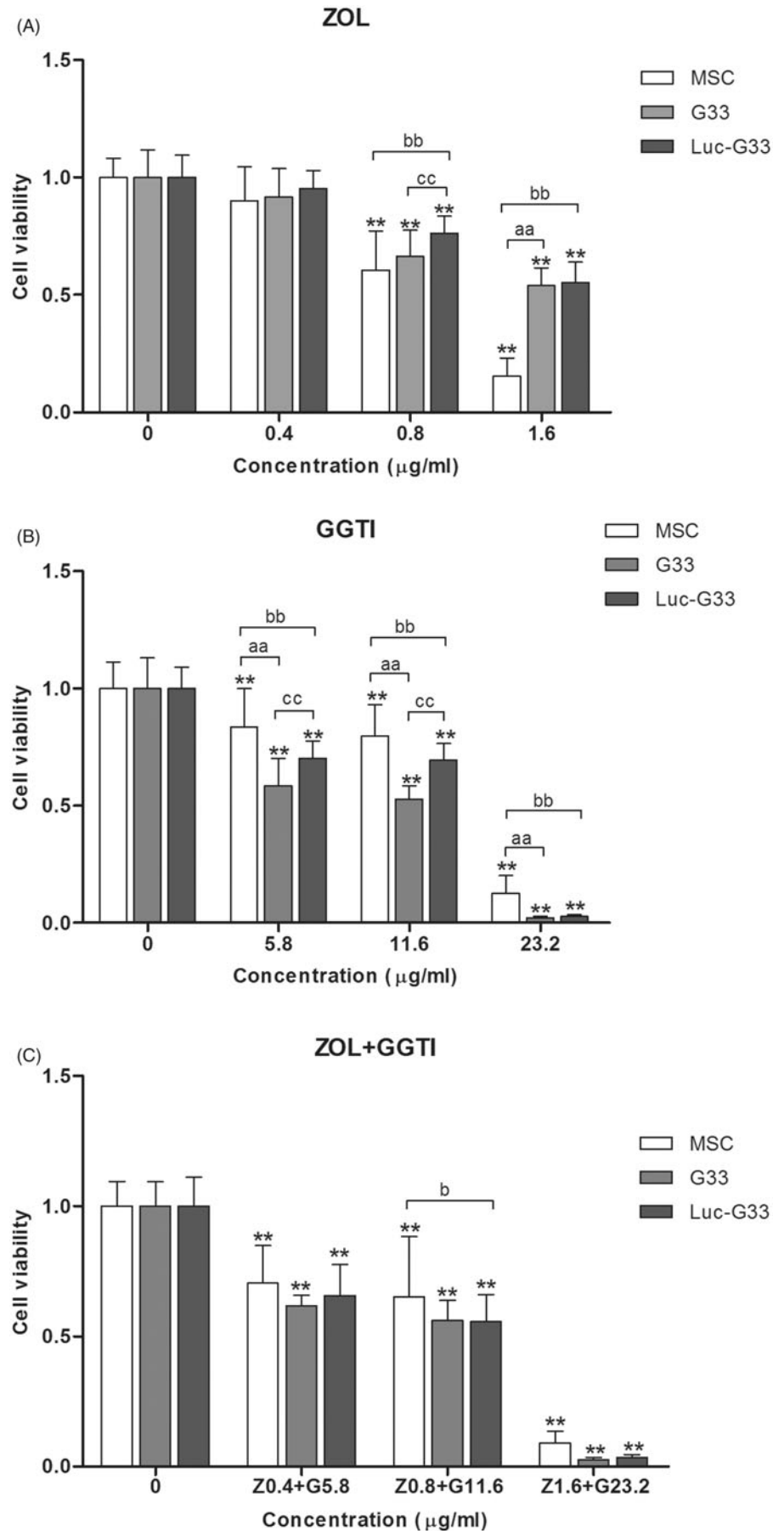
We successfully developed a stable *in vivo* model of GCT stromal cells using luciferase-labeled, primary cultured GCT stromal cells, Luc-G33. This model provided non-invasive and longitudinal investigation of subcutaneous and intraosseous transplantation of GCT stromal cells by BLI. To our knowledge, it is the first *in vivo* model that allows non-invasive and real-time measurement of GCT stromal cell survival and growth after transplantation. In the preliminary study, eight nude mice were injected with Luc-G33 cells subcutaneously under the dorsal skin ( $3 \times 10^6$  cells) and intraosseously into the tibiae ( $1 \times 10^6$  cells); BLI was then performed twice per week from day 3 to 42 after cell-implantation (Figure 4A). BLI values were very high at day 3 with an average radiance of  $2.90 \times 10^6 \pm 1.05 \times 10^6$  p/s/cm<sup>2</sup>/sr and  $1.34 \times 10^7 \pm 3.09 \times 10^6$  p/s/cm<sup>2</sup>/sr for the subcutaneous model and the tibial model, respectively (Figure 4B). BLI values in the subcutaneous model did not show any statistically significant difference from day 3 to day 42. However, BLI values decreased significantly from day 3 in a time-dependent manner in the tibial tumor model (Figure 4B).

### ZOL alone and the co-treatment with GGTI-298 inhibited the growth of Luc-G33 cells in the subcutaneous tumor model

Eight mice per group were treated with either 0.9% saline (Control), ZOL (400  $\mu\text{g/kg}$ ), GGTI-298 (1.16 mg/kg), or the combination of ZOL at 400  $\mu\text{g/kg}$  and GGTI-298 at 1.16 mg/kg, respectively at day 3 post cell transplantation, to determine the effects of single treatment alone and the combined treatment in both the subcutaneous and intraosseous models. Tumor growth under the dorsal skin and in the tibiae were monitored by BLI twice per week from day 3 (before drug administration) to day 35 (Figure 5A). The dorsal skin and the tibia samples were harvested on day 35 post cell transplantation to double check the presence of the Luc-G33 cells and the histological changes of the cells if any. BLI values showed that ZOL treatment alone and the co-treatment of ZOL and GGTI-298 significantly reduced tumor cell viability in the subcutaneous model on day 35 as compared to day 3. The BLI signals decreased from  $7.82 \times 10^6 \pm 4.02 \times 10^6$  and  $1.05 \times 10^7 \pm 1.27 \times 10^6$ , respectively, to  $1.44 \times 10^6 \pm 4.46 \times 10^5$  and  $6.22 \times 10^5 \pm 3.322 \times 10^5$  after treatment with ZOL alone or the co-treatment with ZOL and GGTI-298. There were only 18.41% and 5.95% of the tumor cells survived for ZOL and the co-treatment of ZOL and GGTI-298, respectively. GGTI-298 single treatment

Figure 1. *In vitro* cell viability reduced by (A) ZOL, (B) GGTI-298, and (C) co-treatment with ZOL and GGTI-298 in MSC, G33 and Luc-G33 cells for 5-day, respectively. Data represented the mean and SD of three independent experiments for MTT assay.

\* $p < 0.05$ , \*\* $p < 0.001$  from control by ANOVA and Dunnett's Multiple Comparison Test; aa  $p < 0.001$ , G33 compared with MSC; b  $p < 0.05$ , bb  $p < 0.001$ , Luc-G33 compared with MSC; cc  $p < 0.001$ , G33 compared with Luc-G33, by two-way ANOVA with Bonferroni post-tests.



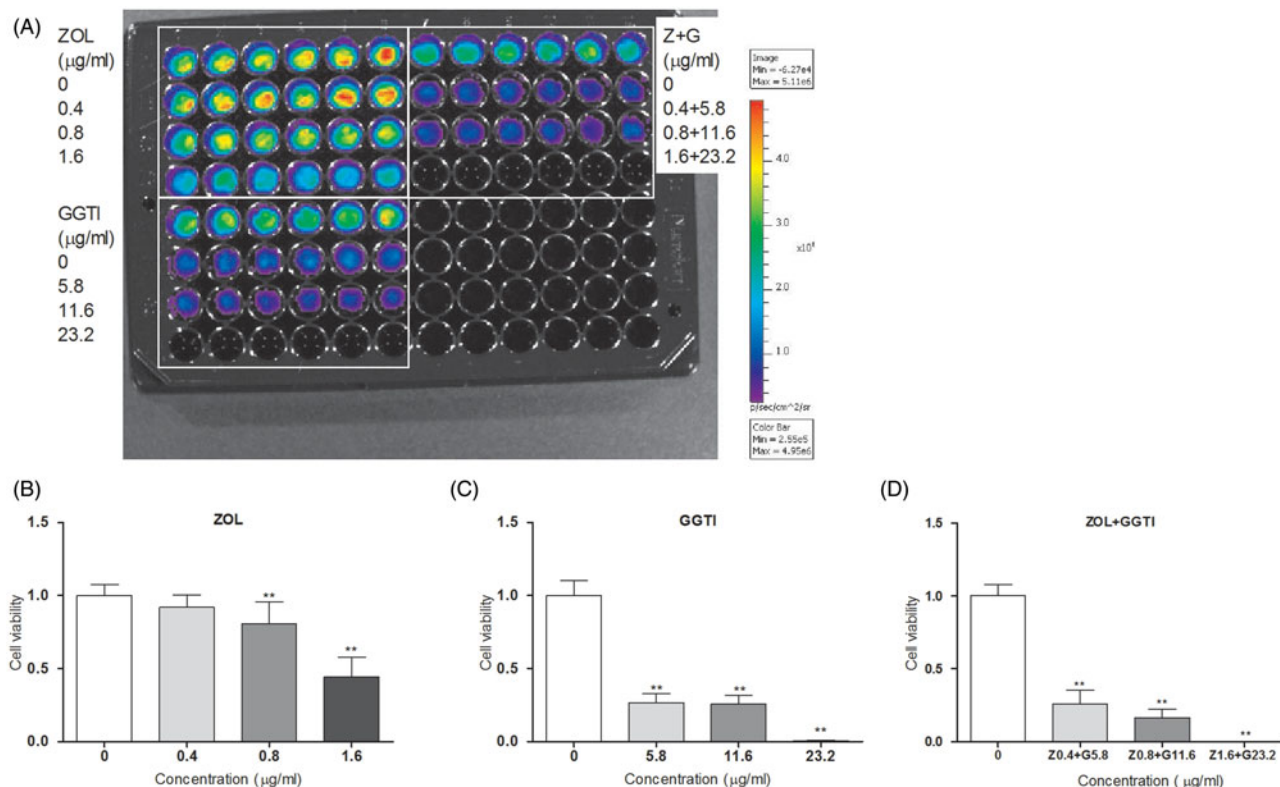


Figure 2. Cell viability measured by luciferase assay and *in vitro* bioluminescent imaging. (A) The diagram showed ZOL, GGTI-298 and the co-treatment of ZOL and GGTI-298 caused a dose-dependent inhibition in cell viability of Luc-G33 cells. Cell viability of Luc-G33 cells were decreased by (B) ZOL, (C) GGTI, and (D) co-treatment with ZOL and GGTI-298. Data represented the mean and SD of three independent experiments for luciferase assay. \* $p < 0.05$ , \*\* $p < 0.001$  from control by ANOVA and Dunnett's Multiple Comparison Test.

resulted in no significant reduction in tumor cell viability in the subcutaneous model (Figure 5B). On the other hand, all treatments except GGTI-298 significantly reduced tumor cell viability in the tibial model (Figure 5C). Since the tumor cell viability decreased significantly even in the control, the inhibitory effects of individual drugs on the tumor cells could not be confirmed by the drugs as they lost viability in the tibial environment.

#### BLI values from the whole body images were correlated with that from tissue samples *ex vivo*

The dorsal skin and the tibia samples injected with Luc-G33 cells were harvested on day 35 and the presence of Luc-G33 cells were confirmed by both the BLI and the immunohistochemistry examinations. BLI values obtained from the whole body images were well correlated with that from the corresponding tissue samples *ex vivo*. The correlation coefficients of BLI values between the whole body images and the tissue samples were 0.62 and 0.60 for the subcutaneous (Figure 6A) and the tibial models (Figure 6B), respectively. Luc-G33 cells grew robustly through the hydrogen gels and showed strong BLI signals in the subcutaneous tumor model in the skin *ex vivo*. On the other hand, Luc-G33 cells were present mainly in the bone marrow in the tibiae *ex vivo* (Figure 6C).

#### Drug treatments suppressed the growth of Luc-G33 in the subcutaneous tumor tissues

The IHC staining data of human mitochondria identification further confirmed the presence of Luc-G33 cells in the skin

(Figure 7A) and tibia tissues (Figure 7C). Relative quantitation of human Luc-G33 cells was evaluated as the percentage of human mitochondria-positive cells, and a significant inhibition was observed in subcutaneous tumors from the mice treated with ZOL ( $16.77 \pm 5.86\%$ ), GGTI-298 ( $10.63 \pm 5.03$ ) or the co-treatment of ZOL and GGTI-298 ( $15.05 \pm 7.72$ ) as compared with the percentage in the control group ( $28.14 \pm 15.96\%$ ; Figure 7B). However, there was no significant difference observed in tibial tumors from the mice treated with ZOL ( $9.20 \pm 5.77\%$ ), GGTI-298 ( $11.54 \pm 8.61$ ) or the co-treatment of ZOL and GGTI-298 ( $11.06 \pm 6.51$ ) as compared with the percentage in the control group ( $10.08 \pm 5.30\%$ ; Figure 7D).

#### Discussion

Previous attempts to create an animal model of GCT wherein there is GCT stromal cells proliferating and osteoclasts mediating bone destruction have not been successful (6–8). In this study, we created an animal model in which GCT stromal cells survived and functioned as proliferating neoplastic cells instead of a GCT model. A highly proliferative cell line of GCT stromal cells was used to create a stable and luciferase-transduced cell line, Luc-G33. Luc-G33 cells exhibited high BLI signal after adding the D-luciferin potassium salt *in vitro*. Although Luc-G33 cells was less sensitive in response to single treatment of ZOL or GGTI-298 than the wild type G33 cells, at medium concentration, no such response was observed in the co-treatment of ZOL and GGTI-298. Moreover, there were no significant differences in the cell

Figure 3. Characterization of the luciferase-transduced GCT stromal cells (Luc-G33 cells) by cell proliferation and recruitment of monocytes. (A) The proliferation rate of the wild type G33 cells and Luc-G33 cells was assessed by BrdU incorporation assay. No significant difference in proliferation rate was observed between G33 and Luc-G33 cells. (B) The recruitment of monocytes by G33 and Luc-G33 cells through a transwell system. No significant difference in the number of monocytes migrated to the lower surface of the transwells with the lower chamber containing G33 or Luc-G33 cells, respectively. Data represented the mean and SD of three independent experiments for BrdU and transwell assays, respectively,  $**p < 0.001$  from control by ANOVA and Dunnett's Multiple Comparison Test.

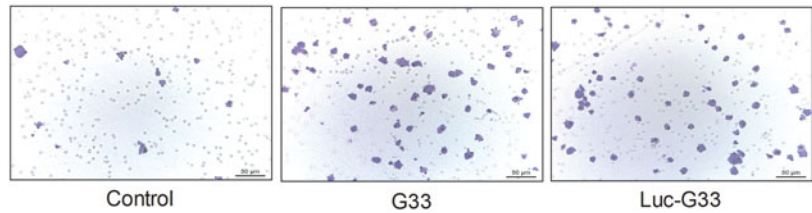
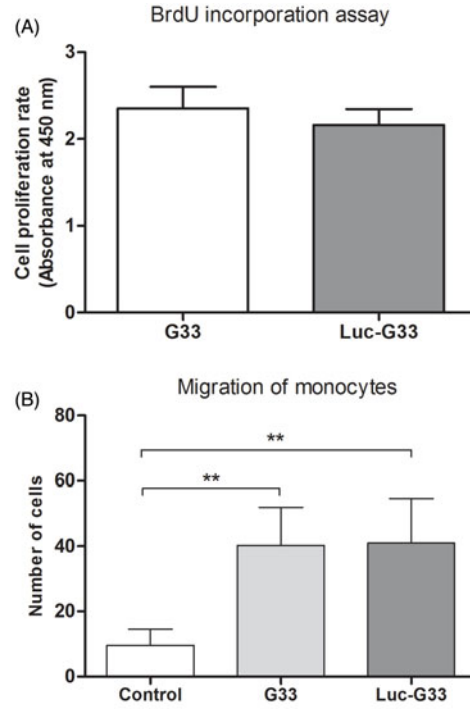
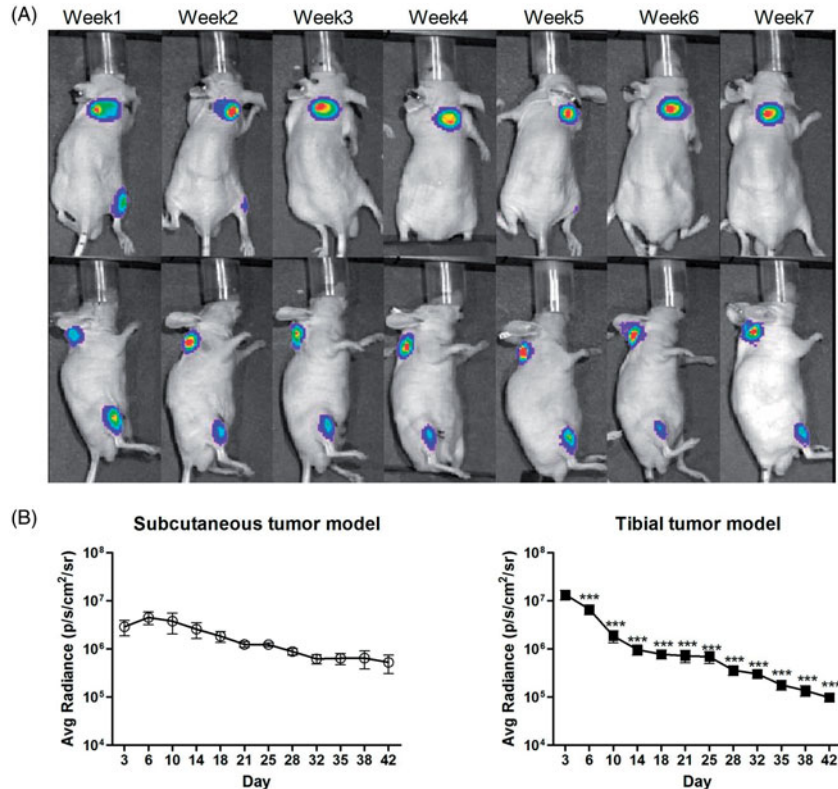


Figure 4. Luc-G33 cells were transplanted into nude mice and the bioluminescent imaging (BLI) was performed twice per week from day 3 to day 42. (A) Representative bioluminescent images from week 1 to 7 showing viable Luc-G33 cells under the dorsal skin and the right tibia of a nude mouse. (B) BLI values from day 3 to 42 in the subcutaneous model and the tibial mode were analyzed by ANOVA and Dunnett's Multiple Comparison Test. Data was plotted on a logarithmic scale as the mean  $\pm$  SEM ( $***p < 0.0001$ ,  $N = 8$ , comparisons between day 3 and all other time points).



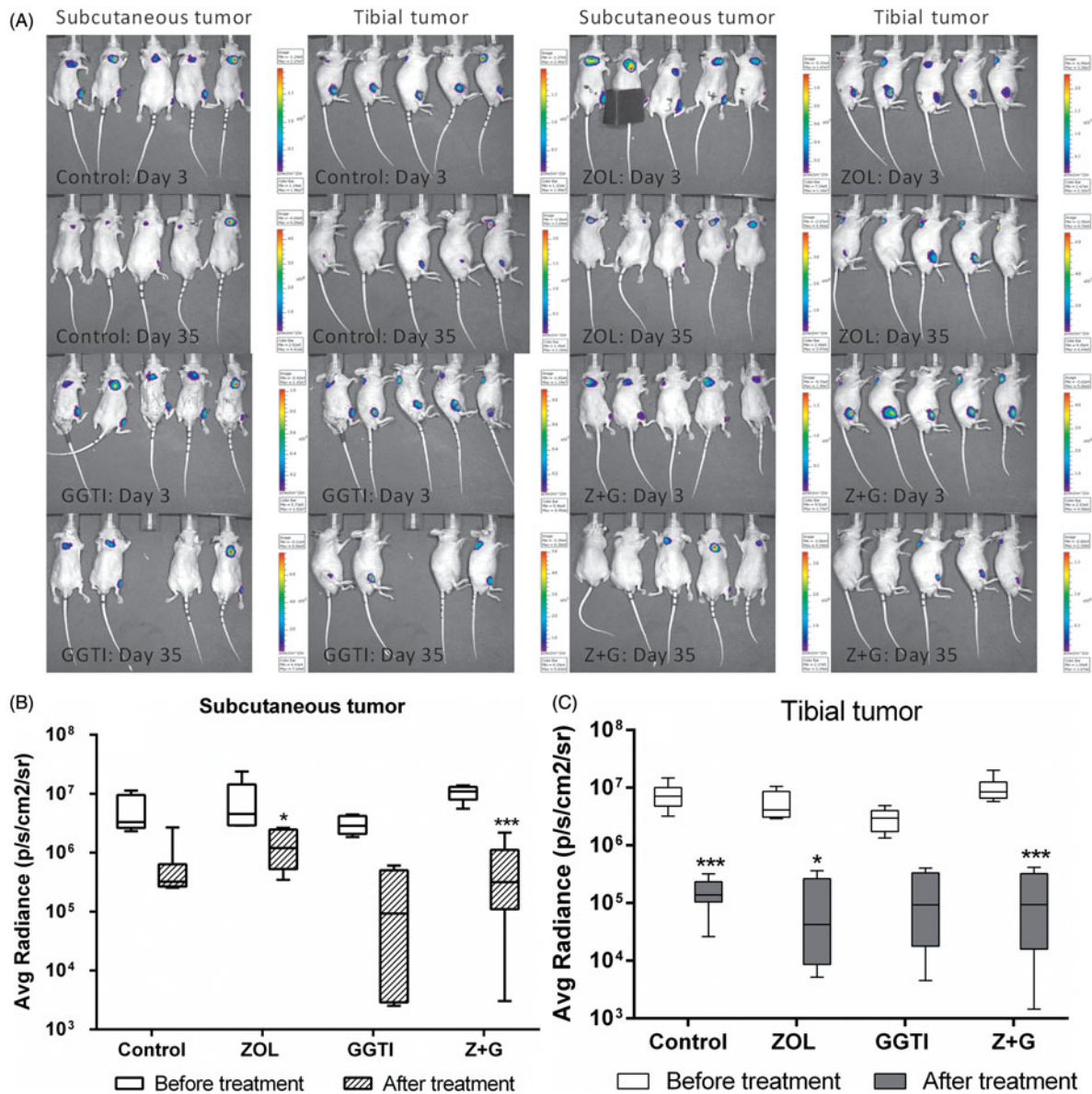


Figure 5. The effects of ZOL (400  $\mu\text{g}/\text{kg}$ ), GGTI-298 (1.16  $\text{mg}/\text{kg}$ ) and the co-treatment on tumor cell viability. (A) Representative BLI of each group assessed on day 3 (before treatment) and day 35 (after treatment). BLI value of each treatment group assessed on day 3 and day 35 in subcutaneous tumor model (B) and in tibial tumor model (C) was analyzed by Two-way ANOVA and Sidak's multiple comparisons test, \* $p < 0.05$ , \*\*\* $p < 0.0001$ ;  $N = 8$  per group. The data in the box and whisker plots represents median, range, and SD.

proliferation rate and the recruitment of monocytes between the wild type G33 cells and Luc-G33 cells, indicating that the luciferase transduction did not much affect the properties and the biological characteristics of GCT stromal cells.

After establishing the stable luciferase-expressing cell line, we used a 3D matrix, extracel-X hydrogel to deliver the Luc-G33 cells either subcutaneously on the back or to the tibiae of the nude mice. Murine RANKL and VEGF were added with the hydrogel to mimic the tumor microenvironment in order to facilitate osteoclast-inducing activity (24,25) and also to suppress the osteoblastic differentiation of the GCT stromal cells in our animal model. The 3D matrix provided a well-contained, growth-enhancing environment in which the tumor cells initially propagated and remained viable on site for 7 weeks in the subcutaneous tumor model. By BLI signal, the Luc-G33 cells were found

to survive for more than 12 weeks in some nude mice (data not shown). However, BLI signals decreased significantly from day 6 after cell implantation in the tibial tumor model. The longer survival of Luc-G33 cells in the subcutaneous tumor model may be associated with a better blood supply due to rapid formation of new microvessels around the tumor. And also, the cell numbers that can be injected into the dorsal skin was three folds more than that into the tibiae. The number of cells injectable into the tibiae is limited by the small volume of the intramedullary space of tibia. This technical limitation may be overcome by drilling two holes in the tibia to drain out some bone marrow and that may provide more space for implanting greater number of tumor cells for better cell survival (26). No matter, the GCT stromal cells only survived in the subcutaneous environment for about 7 weeks, indicating that these cells lose their proliferating capability in the mouse model.

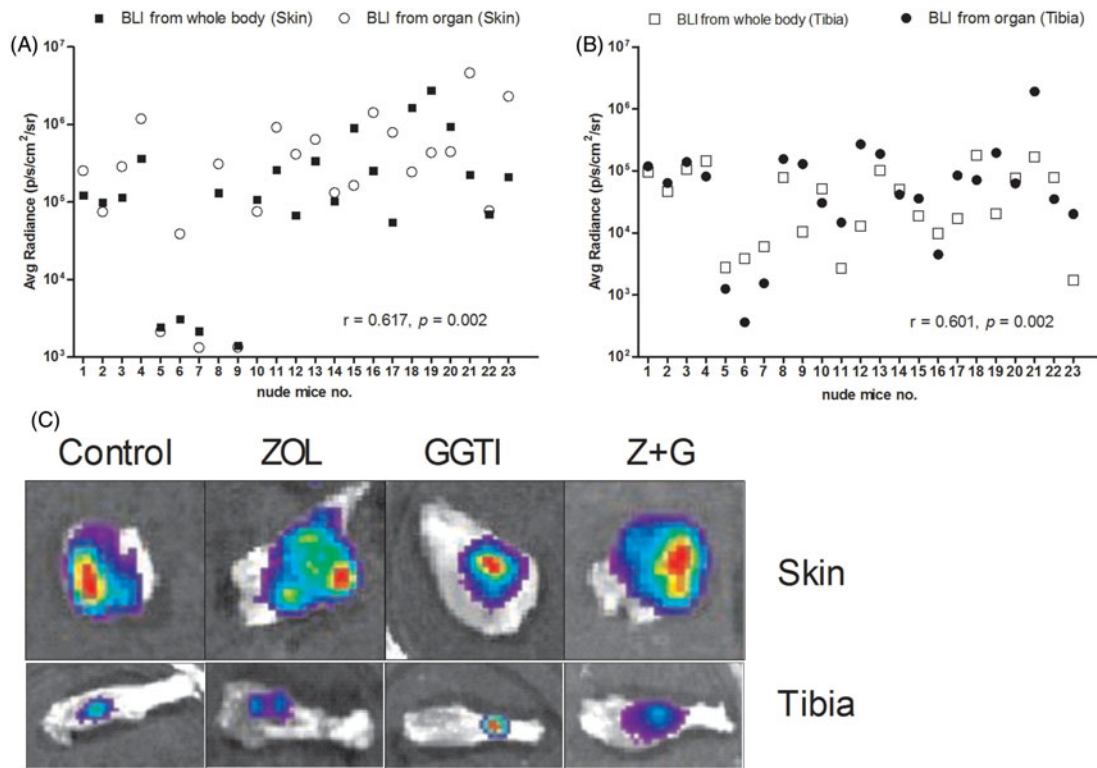


Figure 6. (A,B) The graphs showed BLI values assessed from the whole body images (skin regions and tibia regions) were well correlated with that from the corresponding tissues *ex vivo*. The Spearman correlation coefficients are 0.62 and 0.60 for subcutaneous and tibial regions, respectively,  $N = 23$ ,  $p < 0.01$ . (C) Representative samples from each treatment group showed the presence of Luc-G33 cells in the skins and the tibiae by BLI examination.

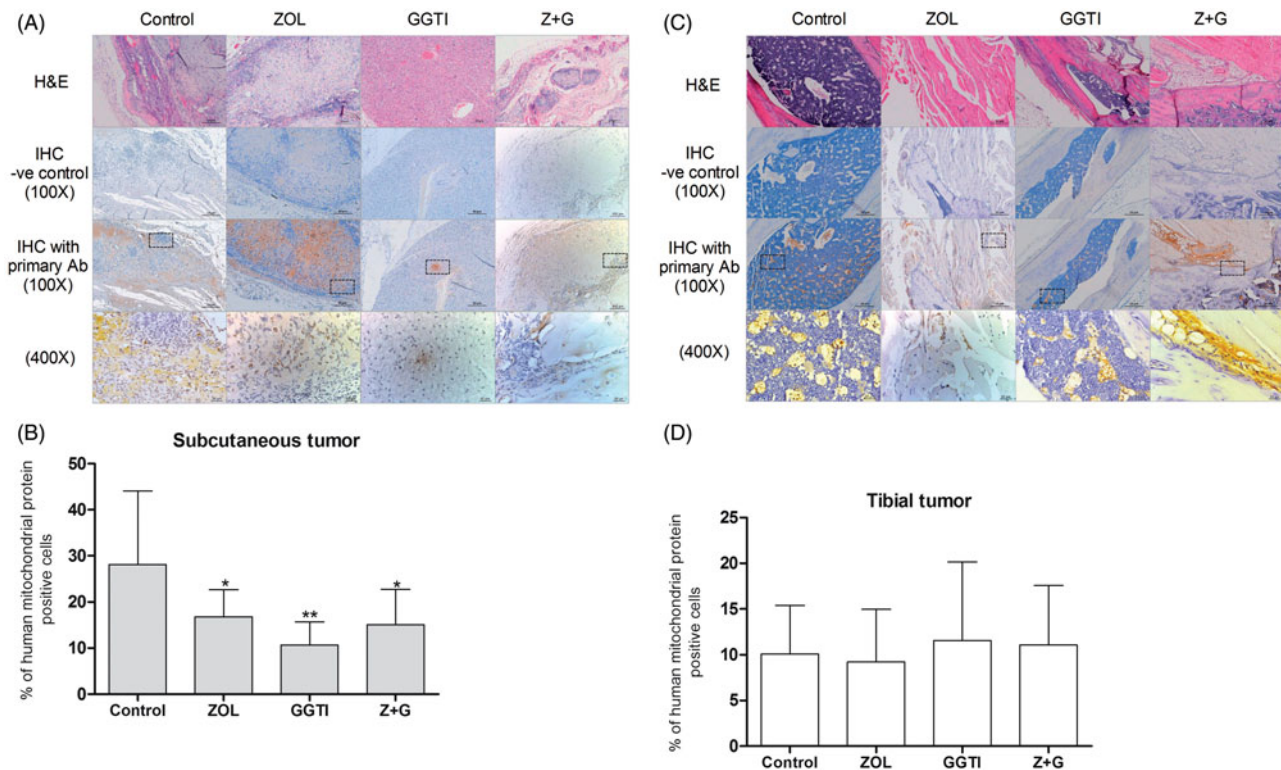


Figure 7. Representative samples from each treatment group showed the histology (H&E) and the presence of Luc-G33 cells in the skins (A) and the tibiae (C), by immunohistochemistry (100 $\times$  magnification). The lowest panel showed magnification ( $\times 4$ ) of the human mitochondria-positive cells (regions of interest) in the upper panel. Luc-G33 cells were stained in brown with anti-human mitochondria antibody. Slides with no primary antibody applied were used for negative controls (the second panel). The graphs showed the percentage of human mitochondria-positive cells under different drug treatments in the subcutaneous tumors (B) and tibial tumors (D), respectively. Assessments were undertaken from two to five tissue samples from each treatment group; \* $p < 0.05$ , \*\* $p < 0.001$  from control by ANOVA and Dunnett's Multiple Comparison Test.

Nitrogen-containing bisphosphonates (N-Bps) are known to inhibit differentiation and induce apoptosis of osteoclasts and certain type of tumor cells by inhibiting the enzyme farnesyl pyrophosphate synthase (FPPS) in the mevalonate pathway. Inhibition of FPPS results in reducing downstream isoprenoid metabolites, farnesyl pyrophosphate (FPP) and geranylgeranyl-pyrophosphate (GGPP) (27) which are essential for prenylation of guanosine triphosphate (GTP)-binding proteins. In addition, protein prenylation inhibitors such as farnesyl transferase inhibitors (FTIs) and geranylgeranyl transferase inhibitors (GGTIs) inhibit the farnesylation and geranylgeranylation respectively of the GTP-binding proteins. Prenylation of such proteins are very important for correct membrane localization and vital cellular functions such as proliferation, differentiation, adhesion and tumorigenesis (28). Therefore, it has been suggested that by combination of N-BPs and FTIs or GGTIs, which exerts multilevel inhibition of the mevalonate and prenylation pathways and may provide a potentially more effective modality for cancer treatment (29).

In this study, we tested the *in vivo* antitumor effects of ZOL and GGTI-298 alone or their combinations in Luc-G33-transplanted nude mice, and assessed by BLI and immunohistochemistry. It was found that ZOL alone at 400 µg/kg and the co-treatment of ZOL at 400 µg/kg and GGTI-298 at 1.16 mg/kg reduced tumor cell viability in the subcutaneous tumor model, whereas, no significant inhibition was found by GGTI-298 treatment alone detected by BLI. In our previous *in vitro* study, we demonstrated that PAM alone reduced cell viability by 52% of the vehicle control and caused S-phase arrest with up-regulation of cyclin D1 protein expression, and the combination of PAM and GGTI-298 significantly reduced cell viability, probably by stimulating caspase-3 activity and inducing cell-cycle S-phase arrest in GCT stromal cells (6). We also demonstrated that ZOL induced a dose-dependent cell inhibition and apoptosis, and reduced cell motility in GCT stromal cells (15). The inhibitory effects of N-BPs and co-treatment with GGTI on GCT stromal cells are confirmed in the present *in vivo* study by the observation of a reduction in BLI signals in the subcutaneous tumor model after ZOL treatment or the co-treatment with GGTI-298. Although a dose-dependent inhibition was observed in Luc-G33 cells *in vitro* by GGTI-289 treatment, no such a dose-dependent response was observed in the present *in vivo* study. The discrepancy between *in vitro* and *in vivo* could be partly explained by different conditions such as supplies of oxygen and nutrients environments, which may cause intrinsic differences in the activities of apoptosis-inducing genes in the tumor cells or differences in their requirements for environment survival factors such as cytokines, or both (30). Nevertheless, relative quantitation of human Luc-G33 cells by IHC staining showed a significant inhibition in subcutaneous tumors from the mice treated with GGTI-298 alone when compared with the control group. The difference between the BLI and IHC staining results may be due to the fact that BLI represents the average of overall signals of the whole tumor tissues, whereas IHC staining only represents a small portion (i.e. 5 µm out of ~1 cm sample) of the whole tumor tissues. In this study, we suggested that BLI gives more accurate and representative results for the *in vivo* drug study as it provides

a longitudinal, continuous assessments of the same tumor tissues in the mice under the whole studying period.

A short-term *in vivo* model of GCT on a chick chorio-allantoic membrane (CAM) has been established by Balke et al. (31). Cell suspensions isolated from GCT tissue were grafted on the CAM for 6 days, solid tumors were formed and composed of human cells interspersed with chick-derived capillaries. This model helps to understand the early phase of tumor seeding, which is an essential step for tumor metastasis or local recurrence. However, the limitation of this model is the short time span (only 6 days) for the tumor growth, which does not allow testing drug effects on animals for longer period of time. Recently, an *in vivo* model of intra-tibial GFP-tagged GCT stromal cells on nude mice has been developed by Ghert et al. (32). This model is a more clinically relevant *in vivo* model which allows assessment of *in vivo* response to therapeutic treatment. Nevertheless, this model does not permit longitudinal, real-time evaluation of tumor burden and inhibition of tumor following drug treatment in the same animals over time. In contrast, our luciferase-transduced GCT stromal cells in an *in vivo* murine model that provides real-time assessments of tumor development and drug effects may have shown advantages over the previous models.

In conclusion, we established a nude mice model of GCT stromal cells which allows non-invasive, real-time assessments of tumor development and testing the *in vivo* effects of different adjuvants for treating GCT. We also demonstrated the inhibitory effects of ZOL treatment alone or the co-treatment with GGTI-298 in GCT stromal cells in the new animal model.

## Acknowledgments

The authors would like to thank Mr. Jimmy Cheng and Dr. Wayne Lee for their assistance in animal experiments.

## Declaration of interest

The authors report no conflicts of interest. This study was supported by the Research Grants Council of the Hong Kong SAR (to Prof. Kumta SM; GRF project no. 466811).

## References

1. Yip MH, Leung PC, Kumta SM. Giant cell tumor of bone. Clin Orthop 1996;323:60–4.
2. Klenke FM, Wenger DE, Inwards CY, Rose PS, Sim FH. Giant cell tumor of bone: risk factors for recurrence. Clin Orthop Relat Res 2011;11:591–9.
3. Niu X, Zhang Q, Hao L, Ding Y, Li Y, Xu H, Liu W. Giant cell tumor of the extremity: retrospective analysis of 621 Chinese patients from one institution. J Bone Joint Surg Am 2012;94:461–7.
4. Tse LF, Wong KC, Kumta SM, Huang L, Chow TC, Griffith JF. Bisphosphonates reduce local recurrence in extremity giant cell tumor of bone: a case-control study. Bone 2008;42:68–73.
5. Balke M, Campanacci L, Gebert C, Picci P, Gibbons M, Taylor R, Hogendoorn P, Kroep J, Wass J, Athanasou N. Bisphosphonate treatment of aggressive primary, recurrent and metastatic Giant Cell Tumour of Bone. BMC Cancer 2010;10:462–9.
6. Lau CP, Huang L, Tsui SK, Ng PK, Leung PY, Kumta SM. Pamidronate, farnesyl transferase, and geranylgeranyl transferase-I inhibitors affects cell proliferation, apoptosis, and OPG/RANKL mRNA expression in stromal cells of giant cell tumor of bone. J Orthop Res 2011;29:403–13.
7. Byers VS, Levin AS, Johnston JO, Hackett AJ. Quantitative immunofluorescence studies of the tumor antigen-bearing cell in

- giant cell tumor of bone and osteogenic sarcoma. *Cancer Res* 1975; 35:2520–31.
8. Oreffo RO, Marshall GJ, Kirchen M, Garcia C, Gallwitz WE, Chavez J, Mundy GR, Bonewald LF. Characterization of a cell line derived from a human giant cell tumor that stimulates osteoclastic bone resorption. *Clin Orthop Relat Res* 1993;296:229–41.
  9. James IE, Dodds RA, Olivera DL, Nuttall ME, Gowen M. Human osteoclastoma-derived stromal cells: correlation of the ability to form mineralized nodules *in vitro* with formation of bone *in vivo*. *J Bone Miner Res* 1996;11:1453–60.
  10. Bauer FCH, Urist MR. The reaction of giant cell tumors of bone to transplantation into athymic nude mice: including observations on osteoinduction in the host bed. *Clin Orthop Relat Res* 1981;159: 257–64.
  11. Joyner CJ, Quinn JM, Triffitt JT, Owen ME, Athanasou NA. Phenotypic characterisation of mononuclear and multinucleated cells of giant cell tumour of bone. *Bone Miner* 1992;16:37–48.
  12. Wulling M, Delling G, Kaiser E. The origin of the neoplastic stromal cell in giant cell tumor of bone. *Hum Pathol* 2003;34: 983–93.
  13. Robinson D, Segal M, Nevo Z. Giant cell tumor of bone. The role of fibroblast growth factor 3 positive mesenchymal stem cells in its pathogenesis. *Pathobiology* 2002;70:333–42.
  14. Lau CP, Ng PK, Li MS, Tsui SK, Huang L, Kumta SM. p63 regulates cell proliferation and cell cycle progression-associated genes in stromal cells of giant cell tumor of the bone. *Int J Oncol* 2013;42:437–43.
  15. Lau CP, Huang L, Wong KC, Kumta SM. Comparison of the anti-tumor effects of denosumab and zoledronic acid on the neoplastic stromal cells of giant cell tumor of bone. *Connect Tissue Res* 2013; 54:439–49.
  16. Chou TC, Talalay P. Quantitative analysis of dose-effect relationships: the combined effects of multiple drugs or enzyme inhibitors. *Adv Enzyme Regul* 1984;22:27–55.
  17. Chou TC. Theoretical basis, experimental design and computerized simulation of synergism and antagonism in drug combination studies. *Pharmacol Rev* 2006;58:621–81.
  18. Lu J, Chan L, Fiji HD, Dahl R, Kwon O, Tamanoi F. *In vivo* antitumor effect of a novel inhibitor of protein geranylgeranyltransferase-I. *Mol Cancer Ther* 2009;8:1218–26.
  19. Zimonjic DB, Chan LN, Tripathi V, Lu J, Kwon O, Popescu NC, Lowy DR, Tamanoi F. *In vitro* and *in vivo* effects of geranylgeranyltransferase I inhibitor P61A6 on non-small cell lung cancer cells. *BMC Cancer* 2013;13:198–207.
  20. Caraglia M, Marra M, Leonetti C, Meo G, D'Alessandro AM, Baldi A, Santini D, Tonini G, Bertieri R, Zupi G, Budillon A, Abbruzzese A. R115777 (Zarnestra)/Zoledronic acid (Zometa) cooperation on inhibition of prostate cancer proliferation is paralleled by Erk/Akt inactivation and reduced Bcl-2 and bad phosphorylation. *J Cell Physiol* 2007;211:533–43.
  21. Buijs JT, Que I, Löwik CW, Papapoulos SE, van der Pluijm G. Inhibition of bone resorption and growth of breast cancer in the bone microenvironment. *Bone* 2009;44:380–6.
  22. Misso G, Porru M, Stoppacciaro A, Castellano M, De Cicco F, Leonetti C, Santini D, Caraglia M. Evaluation of the *in vitro* and *in vivo* antiangiogenic effects of denosumab and zoledronic acid. *Cancer Biol Ther* 2012;13:1491–500.
  23. Tuominen VJ, Ruotoistenmäki S, Viitanen A, Jumppanen M, Isola J. ImmunoRatio: a publicly available web application for quantitative image analysis of estrogen receptor (ER), progesterone receptor (PR), and Ki-67. *Breast Cancer Res* 2010;12(4):R56.
  24. Knowles HJ, Athanasou NA. Hypoxia-inducible factor is expressed in giant cell tumour of bone and mediates paracrine effects of hypoxia on monocyte-osteoclast differentiation via induction of VEGF. *J Pathol* 2008;215:56–66.
  25. Steensma MR, Tyler WK, Shaber AG, Goldring SR, Ross FP, Williams BO, Healey JH, Purdue PE. Targeting the giant cell tumor stromal cell: functional characterization and a novel therapeutic strategy. *PLoS One* 2013;8:e69101.
  26. Deckers M, van Dinther M, Buijs J, Que I, Löwik C, van der Pluijm G, ten Dijke P. The tumor suppressor Smad4 is required for transforming growth factor beta-induced epithelial to mesenchymal transition and bone metastasis of breast cancer cells. *Cancer Res* 2006;66:2202–9.
  27. van beek E, Löwik C, van der Pluijm G, Papapoulos S. The role of geranylgeranylation in bone resorption and its suppression by bisphosphonates in fetal bone explants *in vitro*: a clue to the mechanism of action of nitrogen-containing bisphosphonates. *J Bone Miner Res* 1999;14:722–9.
  28. Appels NM, Beijnen JH, Schellens JH. Development of farnesyl transferase inhibitors: a review. *Oncologist* 2005;10:565–78.
  29. Konstantinopoulos PA, Papavassiliou AG. Multilevel modulation of the mevalonate and protein-prenylation circuitries as a novel strategy for anticancer therapy. *Trends Pharmacol Sci* 2007;28: 6–13.
  30. Kitada S, Andersen J, Akar S, Zapata JM, Takayama S, Krajewski S, Wang HG, Zhang X, Bullrich F, Croce CM, Rai K, Hines J, Reed JC. Expression of apoptosis-regulating proteins in chronic lymphocytic leukemia: correlations with *in vitro* and *in vivo* chemoresponses. *Blood* 1998;91:3379–89.
  31. Balke M, Neumann A, Szuhai K, Agelopoulou K, August C, Gosheger G, Hogendoorn PC, Athanasou N, Buerger H, Hagedorn M. A short-term *in vivo* model for giant cell tumor of bone. *BMC Cancer* 2011;11:241.
  32. Singh S, Singh M, Mak I, Ghert M. Expressional analysis of GFP-tagged cells in an *in vivo* mouse model of giant cell tumor of bone. *Open Orthop J* 2013;7:109–13.